



## Characterizing the effects of shaking intensity on the kinetics of metallic iron dissolution in EDTA

C. Noubactep\*

Angewandte Geologie, Universität Göttingen, Goldschmidtstraße 3, D - 37077 Göttingen, Germany

### ARTICLE INFO

#### Article history:

Received 20 February 2009  
Received in revised form 18 May 2009  
Accepted 19 May 2009  
Available online 22 May 2009

#### Keywords:

Co-precipitation  
EDTA  
Corrosion products  
Reactivity  
Zerovalent iron

### ABSTRACT

Despite two decades of intensive laboratory investigations, several aspects of contaminant removal from aqueous solutions by elemental iron materials (e.g., in  $\text{Fe}^0/\text{H}_2\text{O}$  systems) are not really understood. One of the main reasons for this is the lack of a unified procedure for conducting batch removal experiments. This study gives a qualitative and semi-quantitative characterization of the effect of the mixing intensity on the oxidative dissolution of iron from two  $\text{Fe}^0$ -materials (materials A and B) in a diluted aqueous ethylenediaminetetraacetic solution (2 mM EDTA). Material A (fillings) was a scrap iron and material B (spherical) a commercial material. The  $\text{Fe}^0/\text{H}_2\text{O}/\text{EDTA}$  systems were shaken on a rotational shaker at shaking intensities between 0 and  $250 \text{ min}^{-1}$  and the time dependence evolution of the iron concentration was recorded. The systems were characterized by the initial iron dissolution rate ( $k_{\text{EDTA}}$ ). The results showed an increased rate of iron dissolution with increasing shaking intensity for both materials. The increased corrosion through shaking was also evidenced through the characterization of the effects of pre-shaking time on  $k_{\text{EDTA}}$  from material A. Altogether, the results disprove the popular assumption that mixing batch experiments is a tool to limit or eliminate diffusion as dominant transport process of contaminant to the  $\text{Fe}^0$  surface.

© 2009 Elsevier B.V. All rights reserved.

### 1. Introduction

Iron-based alloys (metallic iron, elemental iron or  $\text{Fe}^0$  materials) have been used as an abiotic contaminant reducing reagent for organic and inorganic groundwater contaminants for over 15 years [1–13]. In this context,  $\text{Fe}^0$  materials are widely termed as zerovalent iron (ZVI) materials, contaminants have been denoted as reductates [14], and the bare surface of  $\text{Fe}^0$  as reductant. The reducing capacity of metallic iron is due to the low standard reduction potential of the redox couple  $\text{Fe}^{\text{II}}/\text{Fe}^0$  ( $E^0 = -0.440 \text{ V}$ ). This makes  $\text{Fe}^0$  a potential reducing agent relative to several redox labile substances, including hydrogen ions ( $\text{H}^+$ ) and oxygen ( $\text{O}_2$ ) [1,15].

Since contaminant reduction by  $\text{Fe}^0$  materials is believed to be surface-mediated, increasing the surface area of the iron, for instance by increasing the amount of  $\text{Fe}^0$  or decreasing the particle size, is believed to increase the rate of the reductive decontamination at the surface of  $\text{Fe}^0$  [15,16]. Based on this seemingly logical premise mechanistic removal studies by  $\text{Fe}^0$  materials have shown that the rate-determining step is electron transfer to the surface-adsorbed molecule [1,17]. There are several arguments against

quantitative contaminant reduction at the  $\text{Fe}^0$  surface; among others the following [18]:

- (i) Huang et al. [19] observed a lag time of some few minutes at pH 4 before nitrate ( $\text{NO}_3^-$ ) reduction took place. The experiments were conducted with  $20 \text{ g L}^{-1}$   $\text{Fe}^0$  (powder) and the solutions were shaken at  $210 \text{ min}^{-1}$ . During these “few minutes” the pH may have increased to values  $>5$  yielding iron oxide precipitates. Iron oxides adsorb  $\text{Fe}^{\text{II}}$  (so called structural  $\text{Fe}^{\text{II}}$ ) and  $\text{NO}_3^-$  such that the observed  $\text{NO}_3^-$  reduction may be mediated by structural  $\text{Fe}^{\text{II}}$ . Clearly, the lag time can be seen as the time necessary for reactive species to be produced.
- (ii) The aqueous corrosion science has unequivocally shown that at  $\text{pH} > 5$  the iron surface is always covered by an oxide film. In this regard Holmes and Meadowcroft [20] described an interesting thumbnail sketch in which without the protective action of a fence (oxide-film) the rabbit ( $\text{Fe}^0$  surface) is a defenceless prey for a rapacious dog (corroding environment). The oxide film generated by corroding  $\text{Fe}^0$  is primary porous. Therefore,  $\text{Fe}^0$  still corrodes after the formation of a surface film. This property is the main characteristic making  $\text{Fe}^0$  materials suitable for environmental remediation.

The presentation above shows clearly that, while “putting corrosion to use” [21], an essential aspect of the iron corrosion was

\* Tel.: +49 551 39 3191; fax: +49 551 399379.  
E-mail address: [cnoubac@gwdg.de](mailto:cnoubac@gwdg.de).

overseen. The main reason for this mistake is that, from the pioneer works on [1,2,17], the reaction vessels have been mixed with the justifiable intention to limit diffusion as a transport mechanism of contaminant to the  $\text{Fe}^0$  surface. However, mixing inevitably increases iron corrosion and depending on the mixing type and the mixing intensity, mixing may avoid/delay the formation of oxide films and/or provoke their abrasion.

The present study investigates the effect of mixing speed on the kinetics of iron dissolution in a system  $\text{Fe}^0/\text{H}_2\text{O}/\text{O}_2/\text{EDTA}$  (simply  $\text{Fe}^0/\text{EDTA}$ ) while the shaking speed varies from 0 to  $250 \text{ min}^{-1}$ . In this system,  $\text{Fe}^0$  is oxidized by dissolved  $\text{O}_2$ ; resulted  $\text{Fe}^{\text{II}}$  and  $\text{Fe}^{\text{III}}$  species are complexed by EDTA. The reactivity of the  $\text{Fe}^0$  material is mainly characterized by the dissolution rate ( $k_{\text{EDTA}}$  in  $\mu\text{g h}^{-1}$  or  $\text{mg h}^{-1}$ ) deduced from the linearity of the iron concentration vs. time curve. The background of this procedure is presented elsewhere [21]. To further characterize  $\text{Fe}^0/\text{EDTA}$  systems, a new parameter is introduced ( $\tau_{\text{EDTA}}$ ). Per definition,  $\tau_{\text{EDTA}}$  for a given system is the time required for the iron concentration to reach 2 mM (112 mg/L). That is the time to achieve saturation assuming 1:1 complexation of  $\text{Fe}^{\text{II,III}}$  by EDTA. To properly characterize the effects of the shaking intensity on the kinetics of iron dissolution ( $k_{\text{EDTA}}$  and even  $\tau_{\text{EDTA}}$ ), two  $\text{Fe}^0$  materials of markedly different reactivity were selected (materials A and B). Material A is a scrap iron from a metal recycling company ("Sorte 69" from Metallaufbereitung Zwickau, Germany) and material B is a commercially available material ("Hartgußstrahlmittel" from Würth, Germany).

## 2. Rationale for use the aqueous $\text{Fe}^0/\text{EDTA}/\text{O}_2$ system

Ethylenediaminetetraacetic acid (EDTA) is a chelating agent that has been used as extracting (dissolving) agent in environmental sciences for decades (Ref. [22] and references therein). The capacity of EDTA to induce and promote the dissolution of iron oxides through surface complex formation that enhance the detachment of the surface metal is well known [23–25]. The driving force for dissolution is the solubility of the oxide phase, which is enhanced by the formation of aqueous  $\text{Fe}^{\text{III}}\text{EDTA}$  complexes. Using this dissolution tool, the reactivity of  $\text{Fe}^0$  materials can be characterized [21].

In investigating the processes of contaminant removal in  $\text{Fe}^0/\text{H}_2\text{O}$  systems EDTA has been used by several researchers [26–29] at concentrations varying from 0 to 100 mM. Thereby, the main goal was to prevent iron oxide precipitation and therefore, eliminate concurrent contaminant adsorption [27] or keep a clean iron surface for contaminant reduction [28]. EDTA was reported to both clean and passivate  $\text{Fe}^0$  materials [26]. The extend and the time scale of occurring of both processes is surely a function of the used EDTA concentration [30]. In a recent study, Gyliene et al. [31] successfully tested  $\text{Fe}^0$  as removing agent for aqueous EDTA.

In an effort to search for an effective, affordable, and environmentally acceptable method for chemical weapon destruction, the potential of the system "zerovalent iron, EDTA and air" (ZEA system) was recently investigated [32–34]. This system generates  $\text{HO}^\bullet$  radicals (in situ) for contaminant oxidation. The ZEA system has several advantages over other systems which have been investigated for the detoxification of organophosphorus compounds (e.g. hydrolysis, palladium-based catalysis, chemical oxidation). Because the ZEA reaction uses inexpensive reagents and proceeds in aqueous solutions, at room temperature and under atmospheric pressure, it can be performed in any laboratory.

This study aims at investigating the short-term kinetics of iron dissolution in ZEA systems while characterizing the effects of shaking intensity on this process. Clearly, a well-documented methodology is used to characterize  $\text{Fe}^0$  reactivity as influenced by the shaking intensity. In this method dissolved oxygen is a reactant and not a disturbing factor. Furthermore since the investigations are

limited to the initial phase of iron dissolution, the possibility that EDTA alters the corrosion process is not likely to be determinant.

## 3. Experimental

### 3.1. Materials

The used iron materials (materials A and B) were selected from 18 materials because of their different reactivity after the EDTA-test [21]. Material A is a scrap iron from a metal recycling company (Metallaufbereitung Zwickau, Germany) containing apart from iron about 3.5% C, 2% Si, 1% Mn and 0.7% Cr. This material was crushed and the size fraction 1.0–2.0 mm was used without further pretreatment. Material B is a spherical (mean diameter = 1.2 mm) commercially available material from Würth (Germany). Material B contained apart from iron about 3.39% C, 0.41% Si, 1.10% Mn, 0.105% S, and 0.34% Cr and was used as received. The specific surface areas were  $0.29 \text{ m}^2 \text{ g}^{-1}$  [35] for material A and  $0.043 \text{ m}^2 \text{ g}^{-1}$  [36] for material B respectively.

### 3.2. Solutions

A standard EDTA solution (0.02 M) from Baker JT<sup>®</sup> (Germany) was used to prepare the working solution. A standard iron solution (1000 mg/L) from Baker JT<sup>®</sup> was used to calibrate the Spectrophotometer. The reducing reagent for  $\text{Fe}^{\text{III}}\text{EDTA}$  was ascorbic acid. 1,10 orthophenanthroline (ACROS Organics) was used as reagent for  $\text{Fe}^{\text{II}}$  complexation. All other chemicals ( $\text{NaHCO}_3$ , L(+)-ascorbic acid, L-ascorbic acid sodium salt, and sodium citrate) used in this study were of analytical grade and all solutions were prepared using Milli-Q purified water.

### 3.3. Iron dissolution experiment

Iron dissolution was initiated by the addition of 0.2 g of the  $\text{Fe}^0$  material to 100 mL of a 2 mM EDTA solution. The experiments were conducted at laboratory temperature (about  $22^\circ\text{C}$ ) in polypropylene Erlenmeyer flask (Nalgene<sup>®</sup>). The Erlenmeyer was placed on a rotary shaker and allowed to react at 0, 50, 100, 150, 200 and  $250 \text{ min}^{-1}$ . The aqueous iron concentration was determined spectrophotometrically with the 1,10 orthophenanthroline method [37,38] using a device from Varian (Cary 50) and recorded as a function of time. The spectrophotometer was calibrated for iron concentration  $\leq 10 \text{ mg/L}$ . Working EDTA-solution (0.002 M) was obtained by one-step dilution of the commercial standard.

At various time intervals, 0.100–1.000 mL (100–1000  $\mu\text{L}$ ) of the solution (not filtrated) were withdrawn from the Erlenmeyer flask with a precision pipette (micro-pipette from Brand<sup>®</sup>) and diluted with distilled water to 10 mL (test solution) in glass essay tubes with 20 mL graduated capacity (the resulted iron concentration was  $\leq 10 \text{ mg/L}$ ). After each sampling, the equivalent amount of distilled water was added to the Erlenmeyer in order to maintain a constant volume.

### 3.4. Dissolution of iron and in situ generated iron corrosion products

To evidence the fact that shaking the reaction vessels yields increased corrosion products (e.g.  $\text{Fe}_3\text{O}_4$ ), 0.2 g of material A was added to 50 mL deionized water and pre-shaken at  $100 \text{ min}^{-1}$  for 0, 3, 6, 18, 30 and 48 h (systems I, II, III, IV, V and VI respectively). Subsequently, 50 mL of an ascorbate buffer was added to the systems (resulting ascorbate concentration: 0.115 M or 115 mM), the systems were further shaken at  $100 \text{ min}^{-1}$ , and the time dependence of the evolution of iron concentration was characterized. Under the experimental conditions (pH 7.6) aqueous iron originates

essentially from two sources: (i) reductive dissolution of corrosion products through ascorbate, and (ii) oxidative dissolution of  $\text{Fe}^0$  through dissolved oxygen. Assuming a 1:1 complexation, the used ascorbate concentration can dissolve 115 mM of iron or 38 mM of magnetite ( $\text{Fe}_3\text{O}_4$ ), that is 8.9 g of corrosion products. Because only 0.2 g of  $\text{Fe}^0$  material (producing maximal 0.28 g of  $\text{Fe}_3\text{O}_4$ ) was used for the experiments, ascorbate was necessarily in excess with respect to the possible amount of corrosion products. It is expected that the amount of dissolved iron will be minimal in the non-pre-shaken system (reference, pre-shaken for 0 h) and increased with increasing pre-shaking time.

### 3.5. Analytical methods

For iron determination, 1 mL of a 0.4 M ascorbate buffer was added to the test solution (10 mL) in the assay tube for  $\text{Fe}^{\text{III}}$  reduction followed by two times 4 mL distilled water for homogenization. Finally, 1 mL of a 1% 1,10 phenanthroline solution was added for  $\text{Fe}^{\text{II}}$  complexation. The serial addition of ascorbate buffer (1 mL), water ( $2 \times 4$  mL) and phenanthroline solution (1 mL) occurred with an appropriated device from Brand® (Handystep). The assay tubes were then sealed, vigorously shaken manually and allowed to react for at least 15 min. The iron concentration was determined at 510 nm on the Spectrophotometer. The kinetics of  $\text{Fe}^0$  oxidative dissolution was investigated by determining the amount of iron in the supernatant solution. The experiments were performed in triplicates. The mean values are presented together with the standard deviation (bares in the figure).

## 4. Results and discussion

### 4.1. Background

The present work characterizes the effects of shaking speed on the rate of iron dissolution ( $k_{\text{EDTA}}$ ) from two  $\text{Fe}^0$ -materials in a 0.002 M EDTA solution. Under the experimental conditions  $\text{Fe}^0$  is oxidized by dissolved  $\text{O}_2$  and resulted  $\text{Fe}^{\text{II}}$  and  $\text{Fe}^{\text{III}}$  species are complexed by EDTA. Ideally, under given experimental conditions, Fe concentration increases continuously with time from  $0 \text{ mg L}^{-1}$  at the start of the experiment ( $t=0$ ) to  $112 \text{ mg L}^{-1}$  (0.002 M) at saturation ( $\tau_{\text{EDTA}}$ ) when a 1:1 complexation of Fe and EDTA occurs. During this period the initial uncoloured solution becomes increasingly yellow. After saturation is reached, Fe concentration may: (i) increase, turning the solution a darker brown colour, (ii) remain constant or (iii) decrease depending on the dominating processes in the bulk solution. For example, if the hydrodynamic conditions are favourable for super-saturation the aqueous iron concentration will increase. If the nucleation is favourable and rapid the iron concentration will decrease more or less rapidly. This study is mainly focussed on processes occurring before the saturation. Thereby, the time-variant iron concentration is likely to be linear. The solutions were not filtered and concentrations above saturation are regarded as being of indicative nature even though the results were reproducible. Clearly, reported iron concentrations may not necessarily reflected dissolved iron. However, it is the aim of this study to show that particulate or colloidal iron is produced by mixing and influence the accessibility of  $\text{Fe}^0$ .

### 4.2. Results

Fig. 1 and Table 1 summarize the results of the kinetics of iron dissolution from the used  $\text{Fe}^0$  materials as the shaking speed varies from 0 to  $250 \text{ min}^{-1}$ . These experiments mostly lasted from 3 to 100 h at all mixing intensities.

The results from Fig. 1 can be summarized as follows.

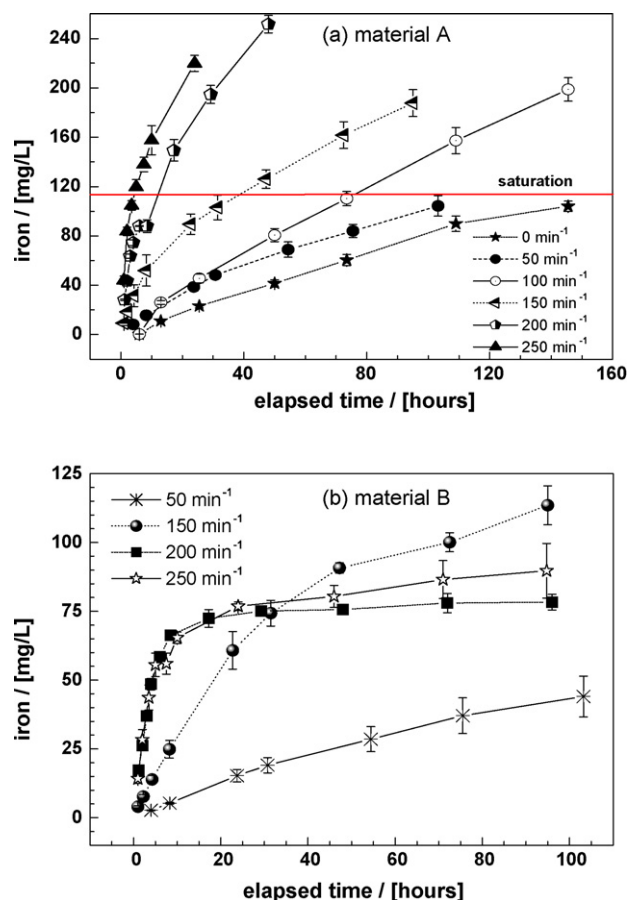


Fig. 1. Evolution of the total iron concentration as a function of time for different shaking intensities from the scrap iron (a) and the commercial material (b). The experiments were conducted in a 2 mM EDTA solution with a material loading of  $2 \text{ g/L}$ . The lines are not fitting functions, they simply connect points to facilitate visualization.

- A 2 mM EDTA solution is efficient at sustaining  $\text{Fe}^0$  (oxidative) dissolution at pH values  $> 5$  (initial pH: 5.2).
- Fe dissolution in 2 mM EDTA is significantly increased by shaking the experimental vessels. The higher the shaking intensity, the higher the dissolution rate.
- The Fe dissolution from material A (Fig. 1a) may yield to Fe saturation at all tested shaking intensities (including  $0 \text{ min}^{-1}$ ).
- Fe saturation for material B (Fig. 1b) was achieved only for a shaking intensity of  $150 \text{ min}^{-1}$  ( $114 \pm 7 \text{ mg L}^{-1}$ ). For higher mixing intensities (200 and  $250 \text{ min}^{-1}$ ) a maximal concentration of about  $80 \text{ mg L}^{-1}$  (70% saturation) was reached. There was no significant difference between the experiments at 200 and  $250 \text{ min}^{-1}$  indicating that increasing the mixing intensity from 200 to  $250 \text{ min}^{-1}$  will not significantly affect material B reactivity.
- For both materials the initial dissolution ( $k_{\text{EDTA}}$ ) was always a linear function of the time; the regression parameters from these functions are given in Table 1.
- For mixing intensities  $> 150 \text{ min}^{-1}$  the linear part of the curve  $[\text{Fe}] = f(t)$ ; is practically parallel to the  $[\text{Fe}]$  axis. This yields to physically meaningless  $b$  values (Table 1).  $[\text{Fe}] = k_{\text{EDTA}} \times t + b$ . Ideally,  $b$  is the concentration of iron at origin. It is per definition the amount of iron dissolved from atmospheric corrosion products, present on  $\text{Fe}^0$  at the beginning of the experiment [21].

The results from Table 1 can be summarized as follows.

**Table 1**  
Effect of shaking speed on the oxidative dissolution of Fe<sup>0</sup> in the presence of 2 × 10<sup>-3</sup> M EDTA (2 mM EDTA). *n* is the number of experimental points for which the curve iron concentration ([Fe]) vs. time (*t*) is linear (Fig. 1). [Fe] = *k*<sub>EDTA</sub> × *t* + *b*; *k*<sub>EDTA</sub> and *b*-values were calculated in Origin 6.0.

Speed (min <sup>-1</sup> )	<i>n</i>	<i>r</i>	<i>k</i> <sub>EDTA</sub> (μg h <sup>-1</sup> )	<i>b</i> (μg)	τ <sub>EDTA</sub> (h)	τ <sub>EDTA</sub> (d)
<b>Material A</b>						
0	5	0.999	83 ± 3	61 ± 57	135	5.61
50	7	0.980	118 ± 11	536 ± 226	90	3.74
100	6	0.999	135 ± 4	926 ± 125	76	3.17
150	7	0.974	218 ± 19	1096 ± 426	46	1.93
200	4	0.997	1775 ± 102	771 ± 184	6	0.24
250	4	0.942	1970 ± 498	3353 ± 1341	4	0.17
<b>Material B</b>						
50	7	0.988	52 ± 4	71 ± 26	213	8.9
150	7	0.995	192 ± 9	264 ± 77	57	2.4
200	5	0.990	898 ± 72	758 ± 204	12	0.5
250	4	0.995	1070 ± 79	415 ± 182	10	0.42

- The dissolution rate (*k*<sub>EDTA</sub>) for material A varies from 83 μg h<sup>-1</sup> at 0 min<sup>-1</sup> (not shaken) to 1970 μg h<sup>-1</sup> (ca. 2 mg h<sup>-1</sup>) at 250 min<sup>-1</sup>. For material B *k*<sub>EDTA</sub> varies from 52 μg h<sup>-1</sup> at 50 min<sup>-1</sup> to 1070 μg h<sup>-1</sup> (ca. 1 mg h<sup>-1</sup>) at 250 min<sup>-1</sup>. This result shows that material A is more reactive in a non-shaken experiment than material B shaken at 50 min<sup>-1</sup>.
- The same trend for *k*<sub>EDTA</sub> was observed for τ<sub>EDTA</sub>. The largest value of τ<sub>EDTA</sub> (213 h or 9 days) was observed for material B shaken at 50 min<sup>-1</sup> and the lowest for material A at 250 min<sup>-1</sup> (4 h). This observation demonstrates the ability of τ<sub>EDTA</sub> to characterize the reactivity of Fe<sup>0</sup> material under various experimental conditions.
- For mixing intensities ≤150 min<sup>-1</sup>, *k*<sub>EDTA</sub> (Fig. 2), *b*-values and τ<sub>EDTA</sub> linearly increased with the mixing speed. A sudden change was observed between 150 and 200 min<sup>-1</sup> for both materials despite the huge reactivity difference (Fig. 2). This material-independent behaviour suggests a change in the hydrodynamic regime. In Fe<sup>0</sup>/H<sub>2</sub>O/contaminant systems, this region at higher mixing intensities is associated with the absence of transport limitations (e.g. Ref. [39]). However, considering the fact that Fe oxyhydroxides precipitate in the system as well, it is possible that contaminant removal at higher mixing intensities is associated with oxide precipitation and not with the iron surface. This conclusion is supported by recent data on methylene blue discoloration in Fe<sup>0</sup>/H<sub>2</sub>O systems [40,41]. Several studies have concluded that Fe<sup>0</sup> transformation reactions are either transport limited [42–44] or reaction limited [45,46]. Since an oxide film is always present on the Fe<sup>0</sup> surface (at pH > 5), diffusion is an

inevitable transport path. Moreover mechanistic investigations should be performed under conditions favouring diffusion [18].

### 4.3. Discussion

As shown above no Fe super-saturation occurs in experiments with material B. In all experiments with this material the solution at the end of the experiment was almost yellow and limpid. On the contrary yellow limpid solutions were observed as end-solutions in experiments with material A only at shaking speeds ≤150 min<sup>-1</sup>. For experiments at 200 and 250 min<sup>-1</sup> a turbid dark-brown coloration was observed some hours after the start of the experiment. Table 2 summarizes some basic equations for corrosion product generation. Simplifying, the observed coloration can be considered as the result of a precipitation reaction between excess Fe<sup>3+</sup> ions (after solution saturation) from iron corrosion and OH<sup>-</sup> ions from O<sub>2</sub> reduction yielding Fe(OH)<sub>3</sub> precipitates (see Table 2, Eqs. (3a), (3b), (6), and (7)). Like all precipitation processes, this reaction is influenced by mixing. Mixing liquids to precipitate solid particles is a common multiphase chemical process that comprises several complex phenomena [47–57].

The reaction between Fe<sup>3+</sup> and OH<sup>-</sup> initially forms soluble Fe(OH)<sub>3</sub>, but in a supersaturated, metastable state relative to its equilibrium solubility product. Comparing the behaviour of both materials it can be stated that the metastability is possible around a shaking speed of 150 min<sup>-1</sup>. This statement is supported by the

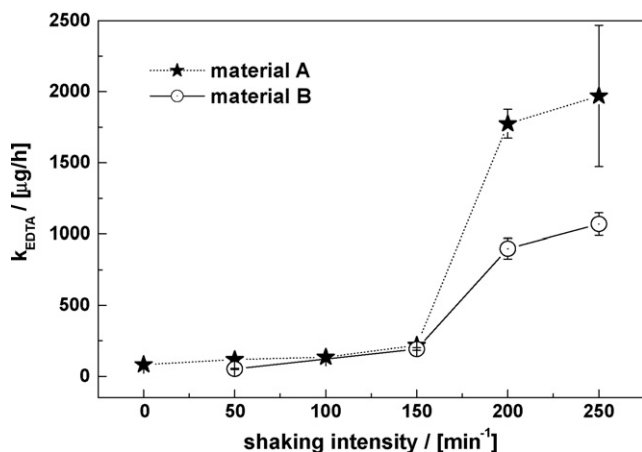


**Fig. 2.** Variation of the rate of iron dissolution (*a* values) as a function of the shaking intensity for the scrap iron (material A) and the commercial material (material B). The lines are not fitting functions, they simply connect points to facilitate visualization.

**Table 2**

Some relevant reactions involved in contaminant removal in the system Fe<sup>0</sup>/H<sub>2</sub>O. Ox is the oxidized contaminant and Red is corresponding non- or less toxic/mobile reduced form. *x* is the number of electrons exchanged in the redox couple Ox/Red. It can be seen that Fe<sup>0</sup> and its secondary (Fe<sup>2+</sup>, H<sub>2</sub>) and ternary (FeOOH, Fe<sub>3</sub>O<sub>4</sub>, Fe<sub>2</sub>O<sub>3</sub>) reaction products are involved in the process of Ox removal.

Reaction equation	
$x\text{Fe}^0 + \text{Ox}_{(\text{aq})} \Rightarrow \text{Red}_{(\text{sor aq})} + x\text{Fe}_{(\text{aq})}^{2+}$	(1) <sup>a</sup>
$2\text{Fe}^0 + \text{O}_2 + 2\text{H}_2\text{O} \Rightarrow 4\text{OH}^- + 2\text{Fe}_{(\text{aq})}^{2+}$	(2)
$\text{Fe}_s^0 + 2\text{H}_2\text{O} \Rightarrow \text{H}_2 + 2\text{OH}^- + \text{Fe}_{(\text{aq})}^{2+}$	(3a)
$2\text{Fe}^0 + 2\text{H}_2\text{O} + \frac{1}{2}\text{H}_2\text{O} \Rightarrow 2\text{FeOOH}$	(3b)
$x\text{H}_2 + 2\text{Ox}_{(\text{aq})} \Rightarrow 2\text{Red}_{(\text{sor aq})} + 2x\text{H}^+$	(4)
$x\text{Fe}_{(\text{sor aq})}^{2+} + \text{Ox}_{(\text{aq})}^* \Rightarrow \text{Red}_{(\text{sor aq})} + x\text{Fe}^{3+}$	(5)
$2\text{Fe}^{2+} + \frac{1}{2}\text{O}_2 + 5\text{H}_2\text{O} \Rightarrow 2\text{Fe}(\text{OH})_3 + 4\text{H}^+$	(6)
$\text{Fe}(\text{O})_3 \Rightarrow \alpha\text{-}, \beta\text{-FeOOH}, \text{Fe}_3\text{O}_4, \text{Fe}_2\text{O}_3$	(7) <sup>a</sup>
$\text{Fe}_2\text{O}_3 + 6\text{H}^+ + 2\text{e}^- \Rightarrow 2\text{Fe}^{2+} + 3\text{H}_2\text{O}$	(8)
$\text{Fe}_2\text{O}_3 + 2\text{H}^+ + 2\text{e}^- \Rightarrow 2\text{Fe}_3\text{O}_4 + \text{H}_2\text{O}$	(9)
$8\text{FeOOH} + \text{Fe}^{2+} + 2\text{e}^- \Rightarrow 3\text{Fe}_3\text{O}_4 + 4\text{H}_2\text{O}$	(10)

<sup>a</sup> Nonstoichiometric.

persistence of the yellow colour at an over-saturation of 70% in the experiment with material A at  $150 \text{ min}^{-1}$  ( $[\text{Fe}] = 188 \pm 11 \text{ mg L}^{-1}$  after 95 h). Note that in the experiment with material B a mixing speed of  $150 \text{ min}^{-1}$  was the only condition where saturation could be achieved. For shaking speeds  $>150 \text{ min}^{-1}$ , either heterogeneous or homogeneous nucleation may have produced stable nuclei that grow into precipitate particles, causing the super-saturation to decline toward its equilibrium value. This is the reason for brownish coloration in experiments with material A where the apparent over-saturation results from suspended particles rather than true super-saturation (the samples were not filtered). In experiments with material B nucleation formation yielded to a stagnation of Fe-concentration at a value of  $80 \text{ mg/L}$ .

If such a system is allowed to age, the increasing stable nucleus size leads to ripening, coarsening of the particulate size distribution, by dissolution of the smallest particles and transfer of their mass to the larger particles [56,58]. Owing to the low solubility of Fe oxyhydroxides, in the absence of a complexing agent ( $\text{pH} > 5$ ) all the processes enumerated above occurred but solely in the vicinity of  $\text{Fe}^0$  materials if the system remains undisturbed. Indeed, mixing affects both the corrosion rate of the bare  $\text{Fe}^0$  surface and the precipitation rate of iron oxides [18]. Prior to any film formation, high mixing rates lead to increased corrosion rates as the transport of cathodic species toward the  $\text{Fe}^0$  surface is enhanced by turbulent transport. At the same time, the transport of  $\text{Fe}^{2+}$  ions away from the  $\text{Fe}^0$  surface is also increased, leading to a lower concentration of  $\text{Fe}^{2+}$  ions at the  $\text{Fe}^0$  surface. This results in a lower surface super-saturation and slower precipitation rate. Both effects account for, that no or less oxide-films are formed at high mixing rates [59].

The results of this study suggest that, while investigating several aspects of contaminant removal by elemental iron, there will be a critical mixing speed (here  $150 \text{ min}^{-1}$ ) above which iron precipitation becomes so fast, that its rate becomes controlled by mixing [55,60]. Under these conditions, segregating the reaction kinetics of the contaminant reductive removal process from the processes associated with Fe oxyhydroxides precipitation (adsorption, co-precipitation) is an impossible issue. Therefore, the argument of a reaction-limited domain at higher mixing rates [37,39,60,61] is questionable. Even under mixing speeds where iron precipitation is moderate, mixing accelerates iron corrosion while avoiding or delaying the formation of corrosion products at the surface of  $\text{Fe}^0$ . This impact of mixing on  $\text{Fe}^0$  materials has been mostly overseen in investigations regarding  $\text{Fe}^0$  for groundwater remediation.

It is interesting to notice that the observed effect of shaking speed on the  $\text{Fe}^0$  reactivity is qualitatively the same as the often-announced effect of mixing intensity on reaction rate constant to demonstrate the possibility of mass-transfer limitations for reactions with elemental metals in batch systems [39]. Thereafter, the overall rate of contaminant reduction by  $\text{Fe}^0$  materials should be mass-transfer limited at slow mixing speeds and reaction-limited at higher mixing speeds. This generally assumed trend is not univocally accepted. As an example, Warren et al. [62] worked with  $\text{Fe}^0$  and  $\text{Zn}^0$  and came to the conclusion that the overall rate of reaction may have been mass-transfer limited in the experiments involving  $\text{Fe}^0$ , and reaction-limited in the  $\text{Zn}^0$  experiments. Concordantly to the results of Warren and co-workers [34,62] and evidences from the open corrosion literature [20,44,63–67], the results of the present study suggest that the rate of contaminant reduction by  $\text{Fe}^0$  materials is always mass-transfer limited. Moreover, the reported reaction mechanism difference at slow and high mixing speeds is likely to be the result of the interference of iron precipitation on the removal process. The products of iron oxide precipitation, whether suspended or settled, necessarily participate to the process of contaminant removal from the aqueous phase. The next section will evidence the increased corrosion at a shaking speed of  $100 \text{ min}^{-1}$ .

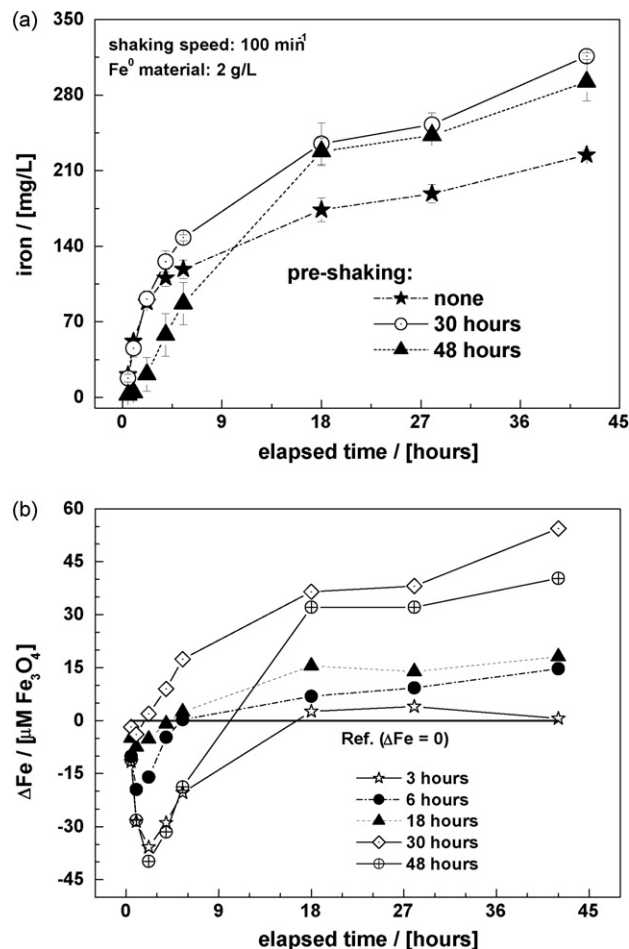


Fig. 3. Effects of the pre-shaking time on the iron dissolution in 0.115 M ascorbate buffer ( $\text{pH} 7.6$ ): (a) kinetics of iron dissolution in the reference system and the systems pre-shaken for 30 and 48 h; (b) excess iron amount ( $\Delta\text{Fe}$ ) as function of the time in all systems in comparison to the reference system. The lines are not fitting functions, they simply connect points to facilitate visualization.

#### 4.4. Evidence of increased corrosion through shaking

The results above confirm the evidence that iron corrodes in water under stagnant and turbulent conditions. Fig. 3 summarizes the results of the evolution of dissolved iron in 0.115 M ascorbate as influenced by pre-shaking operations. It can be seen that the expected trend for the evolution of iron concentration was observed for all systems only for experimental durations  $> 12 \text{ h}$ . For  $t < 12 \text{ h}$  the kinetic of iron dissolution was not uniform. During this period, the evolution of iron concentration in systems IV and V was very comparable to that of the reference system, and systems II, III and VI exhibited lower iron dissolution kinetics. Fig. 3a for instance shows the results for the reference system (system I) and the systems pre-shaken for 30 and 48 h (systems V and VI). It can be seen that in the initial period of the experiment ( $t < 6 \text{ h}$ ), iron dissolution is minimal in system VI (48 h) and very similar in systems I (0 h) and V (30 h). This observation can be attributed to the differential dissolution behaviour of atmospheric corrosion products (system I) and in situ generated corrosion products (systems V and VI) on the one side and the differential dissolution behaviour of in situ generated corrosion products as function of time. The process of aqueous corrosion products generation is known to be complex. For the discussion in this section, it is sufficient to consider that in system V (30 h) a part of corrosion products has a dissolution rate comparable to that of atmospheric products, whereas in system V (48 h) ripening and crystallization processes may have stabilized some

corrosion products, making them more resistant to ascorbate dissolution. Another important behavioural aspect of corrosion products is to limit the accessibility of the Fe<sup>0</sup> surface for dissolved oxygen [66]. From Fig. 3a, it can be seen that after about 12 h, the evolution of the iron concentration is a linear function of the time and that the lines for systems I and V for example are almost parallel. This result indicates that, after the reductive dissolution has freed the Fe<sup>0</sup> surface, dissolved molecular O<sub>2</sub> oxidized Fe<sup>0</sup> uniformly. The distance between the lines of systems I and V is a qualitative reflect of the amount of corrosion products generated during the pre-shaking period. The solubility of the available corrosion products has to be considered as well. This is the reason why more iron dissolved in system V (30 h) than in system VI (48 h).

Fig. 3b shows the results of iron dissolution for all five systems in comparison to the reference system. The excess iron amount in  $\mu\text{m Fe}_3\text{O}_4$  in the individual systems is given as function of the elapsed time. As discussed above it can be seen that in the initial phase of the dissolution experiment, a more or less deficit exists (negative value of  $\Delta\text{Fe}$ ) in all systems, which is primarily attributed to the effects of corrosion products on the availability of Fe<sup>0</sup> for dissolved O<sub>2</sub>. For longer experimental durations, an increased corrosion products generation is observed in all systems. The lack of monotone trend in this increase is attributed to the complex processes accompanying the process of iron corrosion as discussed above.

## 5. Concluding remarks

By quantifying iron oxidative dissolution in 2 mM EDTA under varying mixing speeds, this study has qualitatively evidenced a crucial operational shortcoming associated with the effort to limit the impact of mass transfer while investigating the processes of contaminant removal by Fe<sup>0</sup> materials. In fact, irrespective from the presence of any contaminant, mass transfer of soluble corrosion products (primarily Fe<sup>2+</sup>, Fe<sup>3+</sup> OH<sup>-</sup>, Fe(OH)<sub>2(aq)</sub> and Fe(OH)<sub>3(aq)</sub>) and their precipitation in flowing groundwater is a complex process. While focussing the attention of the behaviour of a selected group of contaminants, most of the existing studies on contaminant removal in Fe<sup>0</sup>/H<sub>2</sub>O systems have felt to adequately consider the interference of corrosion products precipitation [Fe(OH)<sub>2(s)</sub> and Fe(OH)<sub>3(s)</sub>]. The present study discusses the effects of mixing speed on the reactivity of Fe<sup>0</sup> materials and confirms available results from others branches of corrosion science [44,66], that contaminant removal studies should be performed in the mass-transfer controlled regime. Ideally, this regime is achieved under static (non-disturbed) conditions.

Since stagnation is not expected in reactive walls, non-shaken batch experiments do not replicate practical situations. However, this experimental procedure offers a simple tool for the investigation of the impact of oxide-film formation on the contaminant transport to Fe<sup>0</sup> surface. Another promising experimental procedure was proposed by Devlin and Allin [68] and involves the use of a glass-encased magnet reactor in a sealed beaker. In this procedure a granular Fe<sup>0</sup> sample remains stationary while the solution is stirred. In this manner, slowly stirring overcomes the kinetics of mass transfer while corrosion products are not swept from Fe<sup>0</sup> surface. By carefully selecting the stirring speed, real field conditions can be closely simulated.

In light of the results of this study, published results on several aspects of contaminant removal in Fe/H<sub>2</sub>O systems can be reviewed. Thereby, one should try to compare results obtained under comparable mixing regimes. For mechanistic investigations, only results obtained in the mass-transfer controlled regime should be considered. Furthermore, to facilitate comparison of experimental results, the intrinsic material reactivity should be characterized by using the introduced parameter ( $\tau_{\text{EDTA}}$ ). In analogy to iodine number

for activated carbon,  $\tau_{\text{EDTA}}$  can be adopted as standard parameter for Fe<sup>0</sup> characterization. This parameter is facile, cost-effective and does not involve any stringent reaction conditions nor sophisticated laboratory devices. To complete investigations on the mixing effect on Fe<sup>0</sup> reactivity, other mixing types (stirring, bubbling, end-over-end rotating, ultrasonic mixing, vortex) and the impact of reactor geometry should be focussed on. The results of such concerted investigations could be critical  $\tau_{\text{EDTA}}$  values (guide values) at which specific experiments have to be performed. For example, results of Noubactep et al. [41] suggested that, shaking intensities aiming at facilitating contaminant mass transfer to the Fe<sup>0</sup> surface using material A should not exceed 50 min<sup>-1</sup>. Based on this result,  $\tau_{\text{EDTA}} \leq 90$  h (3.75 days) can be adopted as a guide value for the investigation of mass-transfer limited processes. For less reactive Fe<sup>0</sup> materials this critical  $\tau_{\text{EDTA}}$  value will be achieved at shaking intensities >50 min<sup>-1</sup>, but necessarily  $\leq 150$  min<sup>-1</sup> as the hydrodynamics change at 150 min<sup>-1</sup> (Fig. 2). Establishing a small  $\tau_{\text{EDTA}}$  database for the most currently used Fe<sup>0</sup> materials (Fluka filings, Baker chips, Fisher filings, G. Maier GmbH, ISPAT GmbH, Connelly-GPM) can be regarded as an important step toward a broad-based understanding of iron reactive wall technology.

## Acknowledgments

Interesting discussions were held with Dr. T. Licha (Angewandte Geologie, Universität Göttingen) on the spectrophotometric iron determination with o-phenanthroline in the presence of EDTA and are kindly acknowledged. For providing the Fe<sup>0</sup> materials used in this study the author would like to express his gratitude to the branch of the Metallaufbereitung Zwickau Co in Freiberg (Germany) and Dr. R. Köber from the Institute Earth Science of the University of Kiel. M. Rittmeier and R. Pfaar are kindly acknowledged for technical support. The work was supported by the Deutsche Forschungsgemeinschaft (DFG-No 626/2-1).

## References

- [1] L.J. Matheson, P.G. Tratnyek, Reductive dehalogenation of chlorinated methanes by iron metal, *Environ. Sci. Technol.* 28 (1994) 2045–2053.
- [2] R.W. Gillham, S.F. O'Hannesin, Enhanced degradation of halogenated aliphatics by zero-valent iron, *Ground Water* 32 (1994) 958–967.
- [3] S.F. O'Hannesin, R.W. Gillham, Long-term performance of an in situ "iron wall" for remediation of VOCs, *Ground Water* 36 (1998) 164–170.
- [4] T. Bigg, S.J. Judd, Zero-valent iron for water treatment, *Environ. Technol.* 21 (2000) 661–670.
- [5] M.M. Scherer, S. Richter, R.L. Valentine, P.J.J. Alvarez, Chemistry and microbiology of permeable reactive barriers for in situ groundwater clean up, *Rev. Environ. Sci. Technol.* 30 (2000) 363–411.
- [6] J.L. Jambor, M. Raudsepp, K. Mountjoy, Mineralogy of permeable reactive barriers for the attenuation of subsurface contaminants, *Can. Miner.* 43 (2005) 2117–2140.
- [7] A.D. Henderson, A.H. Demond, Long-term performance of zero-valent iron permeable reactive barriers: a critical review, *Environ. Eng. Sci.* 24 (2007) 401–423.
- [8] D.F. Laine, I.F. Cheng, The destruction of organic pollutants under mild reaction conditions: a review, *Microchem. J.* 85 (2007) 183–193.
- [9] A.B. Cundy, L. Hopkinson, R.L.D. Whitby, Use of iron-based technologies in contaminated land and groundwater remediation: a review, *Sci. Total Environ.* 400 (2008) 42–51.
- [10] R.L. Johnson, R.B. Thoms, R.O.B. Johnson, T. Krug, Field evidence for flow reduction through a zero-valent iron permeable reactive barrier, *Ground Water Monit. Remed.* 28 (2008) 47–55.
- [11] R.L. Johnson, R.B. Thoms, R.O.B. Johnson, J.T. Nurmi, P.G. Tratnyek, Mineral precipitation upgradient from a zero-valent iron permeable reactive barrier, *Ground Water Monit. Remed.* 28 (2008) 56–64.
- [12] J. Suk O, S.-W. Jeon, R.W. Gillham, L. Gui, Effects of initial iron corrosion rate on long-term performance of iron permeable reactive barriers: column experiments and numerical simulation, *J. Contam. Hydrol.* 103 (2009) 145–156.
- [13] R. Thiruvengatchari, S. Vigneswaran, R. Naidu, Permeable reactive barrier for groundwater remediation, *J. Ind. Eng. Chem.* 14 (2008) 145–156.
- [14] R. Miehr, P.G. Tratnyek, Z.J. Bandstra, M.M. Scherer, J.M. Alowitz, J.E. Bylaska, Diversity of contaminant reduction reactions by zerovalent iron: role of the reductate, *Environ. Sci. Technol.* 38 (2004) 139–147.
- [15] B. Schrick, J.L. Blough, A.D. Jones, T.E. Mallouk, Hydrodechlorination of trichloroethylene to hydrocarbons using bimetallic nickel-iron nanoparticles, *Chem. Mater.* 14 (2002) 5140–5147.

- [16] T.L. Johnson, M.M. Scherer, P.G. Tratnyek, Kinetics of halogenated organic compound degradation by iron metal, *Environ. Sci. Technol.* 30 (1996) 2634–2640.
- [17] E.J. Weber, Iron-mediated reductive transformations: investigation of reaction mechanism, *Environ. Sci. Technol.* 30 (1996) 716–719.
- [18] C. Noubactep, Processes of contaminant removal in “Fe<sup>0</sup>-H<sub>2</sub>O” systems revisited: the importance of co-precipitation, *Open Environ. J.* 1 (2007) 9–13.
- [19] C.-P. Huang, H.-W. Wang, P.-C. Chiu, Nitrate reduction by metallic iron, *Water Res.* 32 (1998) 2257–2264.
- [20] D.R. Holmes, D.B. Meadowcroft, Physical methods in corrosion technology, *Phys. Technol.* 8 (1977) 2–9.
- [21] C. Noubactep, G. Meinrath, P. Dietrich, M. Sauter, B. Merkel, Testing the suitability of zerovalent iron materials for reactive walls, *Environ. Chem.* 2 (2005) 71–76.
- [22] J. Yu, D. Klarup, Extraction kinetics of copper, zinc, iron, and manganese from contaminated sediment using disodium ethylenediaminetetraacetate, *Water Air Soil Pollut.* 75 (1994) 205–225.
- [23] H.-C. Chang, E. Matijevi, Interactions of metal hydrous oxides with chelating agents. IV. Dissolution of hematite, *J. Colloid Interface Sci.* 92 (1983) 479–488.
- [24] J. Rubio, E. Matijevi, Interactions of metal hydrous oxides with chelating agents. I.  $\beta$ -FeOOH-EDTA, *J. Colloid Interface Sci.* 68 (1979) 408–421.
- [25] J.E. Szecsody, J.M. Zachara, P.L. Bruckhart, Adsorption-dissolution reactions affecting the distribution and stability of Co<sup>II</sup>EDTA in iron oxide-coated sand, *Environ. Sci. Technol.* 28 (1994) 1706–1716.
- [26] T.L. Johnson, W. Fish, Y.A. Gorby, P.G. Tratnyek, Degradation of carbon tetrachloride by iron metal: Complexation effects on the oxide surface, *J. Cont. Hydrol.* 29 (1998) 379–398.
- [27] A. Abdelouas, W. Lutze, H.E. Nutall, W. Gong, Réduction de l’U(VI) par le fer métallique: application à la dépollution des eaux., *C. R. Acad. Sci. Paris: Earth Planetary Sci.* 328 (1999) 315–319.
- [28] J.-L. Chen, S.R. Al-Abed, J.A. Ryan, Z. Li, Effects of pH on dechlorination of trichloroethylene by zero-valent iron, *J. Hazard. Mater.* B83 (2001) 243–254.
- [29] C. Noubactep, Effect of selected ligands on the U(VI) immobilization by zerovalent iron, *J. Radioanal. Nucl. Chem.* 267 (2006) 13–19.
- [30] E.M. Pierce, D.M. Wellman, A.M. Lodge, E.A. Rodriguez, Experimental determination of the dissolution kinetics of zero-valent iron in the presence of organic complexants, *Environ. Chem.* 4 (2007) 260–270.
- [31] O. Gylie, T. Vengris, A. Stoncius, O. Nivinskien, Decontamination of solutions containing EDTA using metallic iron, *J. Hazard. Mater.* 159 (2008) 446–451.
- [32] C. Noradoun, M.D. Engelmann, M. McLaughlin, R. Hutcheson, K. Breen, A. Paszczynski, I.F. Cheng, Destruction of chlorinated phenols by dioxygen activation under aqueous room temperature and pressure conditions, *Ind. Eng. Chem. Res.* 42 (2003) 5024–5030.
- [33] C.E. Noradoun, I.F. Cheng, EDTA degradation induced by oxygen activation in a zerovalent iron/air/water system, *Environ. Sci. Technol.* 39 (2005) 7158–7163.
- [34] C.E. Noradoun, C.S. Mekmaysy, R.M. Hutcheson, I.F. Cheng, Detoxification of malathion a chemical warfare agent analog using oxygen activation at room temperature and pressure, *Green Chem.* 7 (2005) 426–430.
- [35] C. Mbudi, P. Behra, B. Merkel, The effect of background electrolyte chemistry on uranium fixation on scrap metallic iron in the presence of arsenic, Paper Presented at the Inter. Conf. Water Pollut, April 11–13, Natural Porous Media (WAP02), Barcelona, Spain, 2007, 8 pp.
- [36] O. Schlicker, Der Einfluß von Grundwasserinhaltsstoffen auf die Reaktivität und Langzeitstabilität von Fe<sup>0</sup>-Reaktionswänden, Dissertation, Univ. Kiel, 1999, 101 pp.
- [37] L.G. Saywell, B.B. Cunningham, Determination of iron: colorimetric o-phenanthroline method, *Ind. Eng. Chem. Anal. Ed.* 9 (1937) 67–69.
- [38] W.B. Fortune, M.G. Mellon, Determination of iron with o-phenanthroline: a spectrophotometric study, *Ind. Eng. Chem. Anal. Ed.* 10 (1938) 60–64.
- [39] S. Choe, Y.Y. Chang, K.Y. Hwang, J. Khim, Kinetics of reductive denitrification by nanoscale zero-valent iron, *Chemosphere* 41 (2000) 1307–1311.
- [40] C. Noubactep, Characterizing the discoloration of methylene blue in Fe<sup>0</sup>/H<sub>2</sub>O systems, *J. Hazard. Mater.* 166 (2009) 79–87.
- [41] C. Noubactep, A.-M.F. Kurth, M. Sauter, Evaluation of the effects of shaking intensity on the process of methylene 2 blue discoloration by metallic iron, *J. Hazard. Mater.*, in press, doi:10.1016/j.jhazmat.2009.04.046 (Available online 19 April, 2009).
- [42] A. Agrawal, P.G. Tratnyek, Reduction of nitro aromatic compounds by zerovalent iron metal, *Environ. Sci. Technol.* 30 (1996) 153–160.
- [43] S. Nam, P.G. Tratnyek, Reduction of azo dyes with zero-valent iron, *Water Res.* 34 (2000) 1837–1845.
- [44] X. Zhang, X. Tao, Z. Li, R.S. Bowman, Enhanced perchloroethylene reduction in column systems using surfactant-modified zeolite/zero-valent iron pellets, *Environ. Sci. Technol.* 36 (2002) 3597–3603.
- [45] M.M. Scherer, J.C. Westall, M. Ziomek-Moroz, P.G. Tratnyek, Kinetics of carbon tetrachloride reduction at an oxide-free iron electrode, *Environ. Sci. Technol.* 31 (1997) 2385–2391.
- [46] C. Su, R.W. Puls, Kinetics of trichloroethene reduction by zerovalent iron and tin: Pretreatment effect, apparent activation energy and intermediate products, *Environ. Sci. Technol.* 33 (1999) 163–168.
- [47] V.I. Dubodelov, N.M. Kohegura, S.P. Kazachkov, E.A. Markovskii, V.P. Polishchuk, Effect of the hydrodynamic factor on solution of solid metals in molten metals, *Mater. Sci.* 8 (1974) 493–495.
- [48] J.M. Ottino, Mixing, chaotic advection, and turbulence, *Annu. Rev. Fluid Mech.* 22 (1990) 207–253.
- [49] Z. Noszczizus, Z. Bodnar, L. Garamszegi, M. Wittmann, Hydrodynamic turbulence and diffusion-controlled reactions: simulation of the effect of stirring on the oscillating Belousov-Zhabotinskii reaction with the Radicalator model, *J. Phys. Chem.* 95 (1991) 6575–6580.
- [50] T. Arakaki, A. Mucci, A continuous and mechanistic representation of calcite reaction-controlled kinetics in dilute solutions at 25 °C and 1 atm total pressure, *Aquat. Geochem.* 1 (1995) 105–130.
- [51] M.J. Hounslow, H.S. Mumtaz, A.P. Collier, J.P. Barrick, A.S. Bramley, A micro-mechanical model for the rate of aggregation during precipitation from solution, *Chem. Eng. Sci.* 56 (2001) 2543–2552.
- [52] S. Maalej, B. Benadda, M. Otterbein, Influence of pressure on the hydrodynamics and mass transfer parameters of an agitated bubble reactor, *Chem. Eng. Technol.* 24 (2001) 77–84.
- [53] J. Baldyga, L. Makowski, W. Orciuch, Interaction between mixing, chemical reactions, and precipitation, *Ind. Eng. Chem. Res.* 44 (2005) 5342–5352.
- [54] P.E. Dimotakis, Turbulent mixing, *Annu. Rev. Fluid Mech.* 37 (2005) 329–356.
- [55] X. Jiang, Y.G. Zheng, W. Ke, Effect of flow velocity and entrained sand on inhibition performances of two inhibitors for CO<sub>2</sub> corrosion of N80 steel in 3% NaCl solution, *Corr. Sci.* 47 (2005) 2636–2658.
- [56] G. Madras, B.J. McCoy, Mixing effects on particle precipitation, *Ind. Eng. Chem. Res.* 44 (2005) 5267–5274.
- [57] P. Polasek, Differentiation between different kinds of mixing in water purification—back to basics, *Water SA* 33 (2007) 249–252.
- [58] S. Nescic, J.K.-L. Lee, A mechanistic model for carbon dioxide corrosion of mild steel in the presence of protective iron carbonate films—part 3: film growth model, *Corrosion* 59 (2003) 616–628.
- [59] J. Zhang, N. Li, Review of Studies on Fundamental Issues in LBE Corrosion, Los Alamos National Laboratory, 2005.
- [60] D.M. Cwiertny, A.L. Roberts, On the nonlinear relationship between kobs and reductant mass loading in iron batch systems, *Environ. Sci. Technol.* 39 (2005) 8948–8957.
- [61] W.A. Arnold, W.P. Ball, A.L. Roberts, Polychlorinated ethane reaction with zerovalent zinc: pathways and rate control, *J. Contam. Hydrol.* 40 (1999) 183–200.
- [62] K.D. Warren, R.G. Arnold, T.L. Bishop, L.C. Lindholm, E.A. Betterton, Kinetics and mechanism of reductive dehalogenation of carbon tetrachloride using zerovalence metals, *J. Hazard. Mater.* 41 (1995) 217–227.
- [63] M. Cohen, The formation and properties of passive films on iron, *Can. J. Chem.* 37 (1959) 286–291.
- [64] U.R. Evans, *Metallic Corrosion, Passivity and Protection*, Longmans, Green & Co., New York, NY, 1948.
- [65] H. Klas, H. Steinrath, *The Corrosion of Iron and his Protection*, Stahleisen Düsseldorf, 1974 (in German).
- [66] M. Stratmann, J. Müller, The mechanism of the oxygen reduction on rust-covered metal substrates, *Corros. Sci.* 36 (1994) 327–359.
- [67] E.J. Caule, M. Cohen, The formation of thin films of iron oxide, *Can. J. Chem.* 33 (1955) 288–304.
- [68] J.F. Devlin, K.O. Allin, Major anion effects on the kinetics and reactivity of granular iron in glass-encased magnet batch reactor experiments, *Environ. Sci. Technol.* 39 (2005) 1868–1874.